



Controllability of Structural, Optical and Electrical Properties of Ga doped ZnO Nanowires Synthesized by Physical Vapor Deposition

Sang Yeol Lee[†]

Department of Semiconductor Engineering, Cheongju University, Cheongju 360-764, Korea

Received March 5, 2013; Revised March 24, 2013; Accepted April 11, 2013

The control of Ga doping in ZnO nanowires (NWs) by physical vapor deposition has been implemented and characterized. Various Ga-doped ZnO NWs were grown using the vapor-liquid-solid (VLS) method, with Au catalyst on c-plane sapphire substrate by hot-walled pulsed laser deposition (HW-PLD), one of the physical vapor deposition methods. The structural, optical and electrical properties of Ga-doped ZnO NWs have been systematically analyzed, by changing Ga concentration in ZnO NWs. We observed stacking faults and different crystalline directions caused by increasing Ga concentration in ZnO NWs, using SEM and HR-TEM. A D^x peak in the PL spectra of Ga doped ZnO NWs that is sharper than that of pure ZnO NWs has been clearly observed, which indicated the substitution of Ga for Zn. The electrical properties of controlled Ga-doped ZnO NWs have been measured, and show that the conductance of ZnO NWs increased up to 3 wt% Ga doping. However, the conductance of 5 wt% Ga doped ZnO NWs decreased, because the mean free path was decreased, according to the increase of carrier concentration. This control of the structural, optical and electrical properties of ZnO NWs by doping, could provide the possibility of the fabrication of various nanowire based electronic devices, such as nano-FETs, nano-inverters, nano-logic circuits and customized nano-sensors.

Keywords: ZnO, Nanowire, Doped nanowire

1. INTRODUCTION

ZnO is a promising material, which has transparent, piezo-electric, wide-band gap (3.4 eV) and high exciton binding energy (60 meV), for application in electronics and optoelectronics devices. It has been extensively used for light emitting devices (LEDs), nano generator and laser diodes (LDs) using optical characteristics, such as short wavelength and wide band gap [1-5]. ZnO has n-type property due to native defects, such as oxygen vacancies and Zn interstitials. But these characteristics can be varied depending on processing conditions, such as pressure

and temperature, between insulating and conducting properties [6,7]. Also, doping is one of the powerful methods to control electrical properties. In particular, doping controls have already been reported to change the behavior from n-type to p-type, by using various doping materials in thin film [8-11]. However, the doping has been limited, due to restrictive volume and native one-dimensional structure in nanostructures [12]. So, many researchers have studied doping problems of nanowires (NWs). Yuan et al. reported a controlled growth and doping process of well-aligned Ga doped ZnO NWs [13]. Also, M. Sakurai et al. reported electrical transfer properties of Ga doped ZnO NWs with NW FET fabrication [14]. Above these works, Ga doped ZnO NWs were fabricated by chemical vapor deposition (CVD) method, which is not so easy to control, and complicated to fabricate NWs [15]. Therefore, we have used the physical vapor deposition (PVD) method, like hot-walled pulsed laser deposition (HW-PLD), which is a relatively simple process for the application of electronics and optoelectronics devices, compared with CVD

[†] Author to whom all correspondence should be addressed:
E-mail: sylee@cju.ac.kr

Copyright ©2013 KIEEME. All rights reserved.

This is an open-access article distributed under the terms of the Creative Commons Attribution Non-Commercial License (<http://creativecommons.org/licenses/by-nc/3.0>) which permits unrestricted noncommercial use, distribution, and reproduction in any medium, provided the original work is properly cited.

[16]. Also, this process can easily be used to adjust the composition of NWs, by controlling the element component of targets. However, there could be a lot of defects and difficulties of uniform doping in fabricated doped NWs by PVD.

In this paper, we have fabricated Ga doped ZnO NWs with various concentrations (pure, 1 wt%, 3 wt%, and 5 wt%), by using the HW-PLD method. We observed that the Ga dopants had been successfully controlled in ZnO crystal lattice, by using optical and electrical measurements. Based on these results, we demonstrate that physical vapor deposition is simple and efficient to fabricate tunable Ga doped ZnO NWs, and presents systematic control of Ga doping into ZnO NWs.

2. EXPERIMENTS

ZnO NWs were fabricated using the vapor-liquid-solid (VLS) mechanism, by a self-designed HW-PLD. Figure 1 shows a schematic diagram of the HW-PLD system. It is very simple and powerful to fabricate the NWs, which have the same material composition as the target. Moreover, this fabrication system does not require any chemical reactions in the chamber. Therefore, it is very easy to fabricate NWs, without any complex source materials and source tool. In order to control the Ga concentration in ZnO NWs, we used 0 wt%, 1 wt%, 3 wt% and 5 wt% Ga doped ZnO targets with ball-milling the ceramic powders (ZnO and Ga₂O₃), followed by the isostatic press and sintering process [17]. These targets were irradiated by excimer laser, with the operating condition of 248 nm, 1.5 J/cm² and 10 Hz. A target holder was rotated at 4 rpm during the deposition, to prevent cone formation, and to ensure uniform ablation of the target. The Au catalyst thin film was deposited 2 nm on c-plane sapphire substrate by thermal evaporation. Then, ZnO NWs were fabricated at 800 °C for 30 minutes. The NW fabrication pressure was maintained at 1.2 torr. Constant streams of Ar (90 sccm) gases flowed in the furnace during ZnO NWs fabrication. Substrates were located at 2 to 3 cm from the target. The crystalline direction and morphology of as-grown Ga-doped ZnO NWs were analyzed, by using X-ray diffraction (XRD), field emission scanning electron microscope (FE-SEM) and high resolution transmission electron microscopy (HR-TEM), respectively. The optical properties of Ga-doped ZnO NWs were measured by using photoluminescence (PL), depending on temperature. Also, in order to measure electrical properties, as-grown ZnO NWs were suspended in isopropyl alcohol, and dispersed on oxidized Si substrates. Finally, electrodes were fabricated, by using conventional photo-lithography process and e-beam lithography. Ti (10 nm) and Au (180 nm) were deposited, by using electron beam deposition and thermal evaporation, respectively. Fabricated Ga-doped ZnO NW devices were analyzed by using a semiconductor parameter analyzer.

3. RESULTS AND DISCUSSION

Figure 2 shows FE-SEM images of as-grown (a) undoped, (b) 1 wt%, (c) 3 wt%, and (d) 5 wt% Ga doped ZnO NWs. The diameter and the length of these ZnO NWs were 80 to 100 nm, and approximately 10 μm, respectively. As shown in Fig. 2, we observed that all of ZnO NWs had Au particle at the top of NWs. This result clearly indicates VLS growth of ZnO NWs. It is interesting to note that stacking faults have been observed in 1 wt%, 3 wt%, and 5 wt% Ga doped ZnO NWs, different from undoped ZnO NWs. As Ga concentration was increased, the stacking faults also increased, and were much denser, mainly due to the induced stress caused by the different lattice parameters between Zn and Ga. More detailed analysis will be added later, by using HR-TEM.

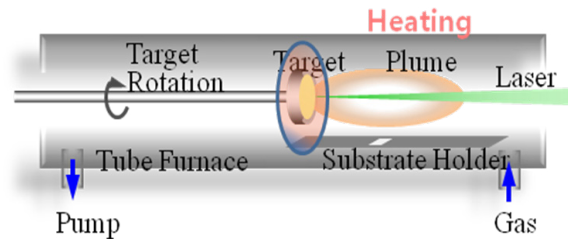


Fig. 1. Schematic diagram of the hot-walled PLD system used in the ZnO NW growths.

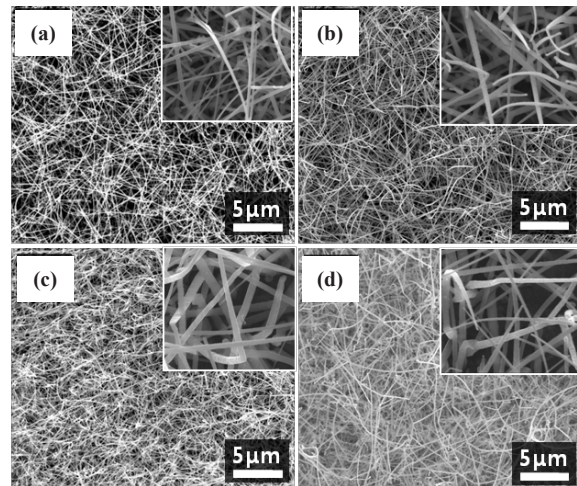


Fig. 2. FE-SEM images of various ZnO-based NWs with (a) undoped, (b) 1 wt%, (c) 3 wt%, and (d) 5 wt% Ga-doped ZnO NWs. Arrow indicates the Au nano-particle at the end of nanowire. Arrow in the inset indicates Au catalyst droplet at the end of NWs.

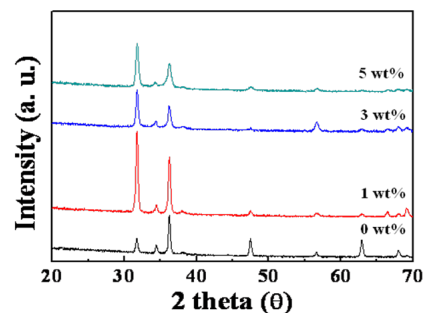


Fig. 3. X-ray diffraction of undoped, 1 wt%, 3 wt% and 5 wt% Ga doped ZnO NWs.

We have examined the structural effect of various Ga concentration in ZnO NWs on the crystallization of ZnO NWs, using XRD. Figure 3 shows the crystalline direction of (a) undoped (b) 1 wt%, (c) 3 wt%, and (d) 5 wt% Ga doped ZnO NWs in the XRD pattern. Pure ZnO NWs mainly grew (100), (002) and (101) planes, of which (100) and (101) planes showed the dominant intensity. The absence of the (002) peak in the XRD pattern was explained by the texture of the film, where most of the wires lay on the plane of the substrate [18]. It is interesting to note that the peak of the (002) plane has disappeared gradually, as Ga concentration increased, and the peak intensity of the (100) plane that was weak in pure ZnO NWs has been gradually stronger. Furthermore, as Ga concentration increased, the (002) plane showed

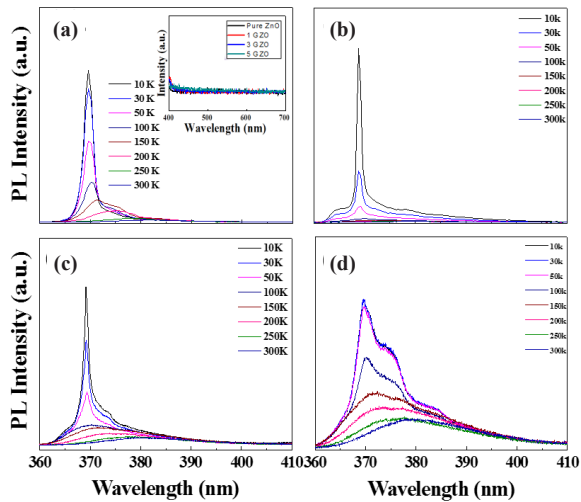


Fig. 4. Photoluminescence spectra of (a) undoped, (b) 1 wt%, (c) 3 wt%, and (d) 5 wt% Ga-doped ZnO NWs. The inset shows photoluminescence spectra of the defect range.

a broad peak. The full width at half maximum (FWHM) of the (002) plane of undoped, 1 wt%, 3 wt% and 5 wt% Ga doped ZnO NWs has been calculated to be about 0.4° , 0.42° , 0.66° and 0.71° , respectively. As shown in SEM images, XRD results also indicated a lattice distortion, due to the introduction of other elements, which had different lattice parameters.

We also investigated the optical properties of ZnO NWs. Figure 4 shows the PL spectra of (a) undoped, (b) 1 wt%, (c) 3 wt%, and (d) 5 wt% Ga doped ZnO NWs, depending on the measurement temperature. The band edge emission of Ga doped ZnO NWs was shifted in the blue direction, compared with undoped ZnO NWs. These results are ascribed to the Burstein-Moss effect, which occurs at a wider optical band gap, because of the difference of effective mass on increasing carrier concentration [19,20]. As shown in the inset of Fig. 4(a), all of the ZnO NWs had dominant band edge emission, without any defects emission. These results indicated that the Ga dopants occupied defect sites in the ZnO NW [14]. So, the band edge emission of these ZnO NWs were sharp, and of high intensity. For 5 wt% Ga doped ZnO NWs, the band edge emission was showed broad and low intensity. At low temperature of 10K, PL spectra of various Ga doped ZnO NWs have been separated into individual emission peaks. Donor-bound exciton emission was clearly observed at all of the Ga doped ZnO NWs. These results represented successful n-type Ga-doping status in ZnO NWs.

Figure 5 shows the HR-TEM images of (a) undoped, (b) 1 wt%, (c) 3 wt%, and (d) 5 wt% Ga doped ZnO NWs. All of the ZnO NWs have been observed to be single crystal-like, by using selected-area electron diffraction (SAED) patterns. Undoped ZnO NW has a wurtzite structure grown along the [001] direction, and smooth surface. The growth direction of Ga doped ZnO NWs has been observed to be changed, by using XRD results. The Ga concentration in ZnO NW induced stress between the Ga dopant and the original lattice element. We observed clearly the stacking faults of Ga doped ZnO NWs in Fig. 5. The covalent bond lengths of Ga-O and Zn-O were 1.92 \AA and 1.97 \AA , respectively. So, accumulated stress induced by the difference of the covalent bond lengths between Ga-O and Zn-O causes the stacking faults, in order to relax the induced stress. The density of stacking faults in undoped, 1 wt%, 3 wt% and 5 wt% Ga doped ZnO NWs were 0 cm^{-1} , $3.03 \times 10^3 \text{ cm}^{-1}$, $6.67 \times 10^3 \text{ cm}^{-1}$ and $1.25 \times 10^4 \text{ cm}^{-1}$, respectively. When the Ga concentration increased in ZnO NWs, the stacking faults were

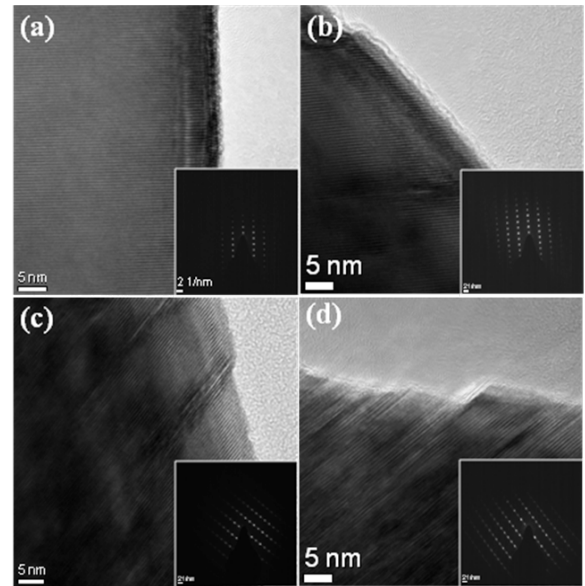


Fig. 5. HR-TEM images of (a) undoped, (b) 1 wt%, (c) 3 wt%, and (d) 5 wt% Ga-doped ZnO NWs.

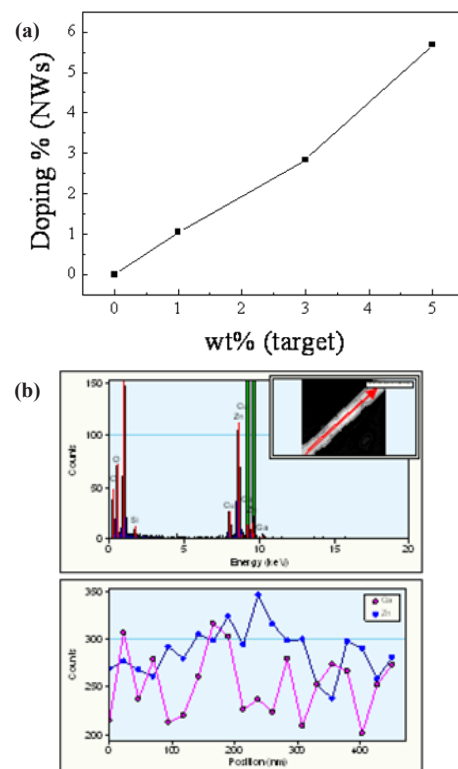


Fig. 6. EDX spectra of (a) undoped, (b) 1 wt%, (c) 3 wt%, and (d) 5 wt% Ga-doped ZnO NWs.

shorter and denser. In particular, 5 wt% doped ZnO NWs had a lot of stacking faults, due to strong stress by different covalent bond length.

Also, we measured the EDS spectrum, in order to confirm the Ga ratio in ZnO NWs. As shown in Fig. 6(a), the Ga ratio at undoped, 1%, 3% and 5 wt% Ga doped ZnO NWs was 0 wt%, 1.05 wt%, 2.84 wt% and 5.69 wt%, respectively. We confirmed that the Ga concentrations in ZnO NWs were successfully controlled by

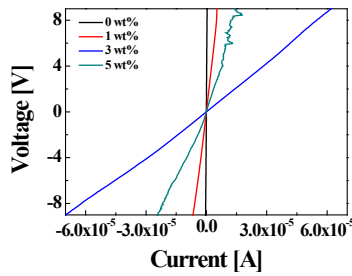


Fig. 7. Typical I-V curve of undoped, 1 wt%, 3 wt% and 5 wt% Ga-doped ZnO NWs.

the physical vapor deposition method, using different ZnO targets, with Ga dopants from 0 wt% to 5 wt%. Figure 6(b) shows the result of the line profile of EDX to confirm uniform distribution of the Ga dopant in 5 wt% Ga doped ZnO NW along the growth direction. It has been confirmed that Ga dopants into in ZnO NWs were observed uniformly in all of the positions, and the average mean counts of Ga dopants per position (nm) were about 255.

Electrical properties of undoped 1 wt%, 3 wt% and 5 wt% Ga doped ZnO NWs were examined, by using semiconductor parameter analyzer. I-V curves of ZnO NWs, as depicted in Fig. 7, confirmed the resistance variation as increasing Ga concentration in the ZnO NWs. The resistance of undoped, 1 wt%, 3 wt% and 5 wt% Ga doped ZnO NWs was 22.13 MΩ, 1.30 MΩ, 0.13 MΩ and 0.39 MΩ, respectively. The resistance of Ga doped ZnO NWs from undoped to 3 wt% clearly decreased by one order. From these results, it could be understood that Ga dopants were successfully doped into ZnO NWs, resulting in the generation of donor carriers, which reduced the resistance, when the Ga concentration increased up to 3 wt% in ZnO NWs. However, 5 wt% Ga doped ZnO NW had a lot of Ga concentration, which induced the decrease of mean free path of the carrier [21]. Consequently, it could be suggested that the resistance of heavily doped ZnO NW increased slightly, due to the increase of scattering. For more detail of the electrical properties, we have attempted to fabricate various Ga doped ZnO NW FETs. However, it was very hard to observe the off-state in Ga-doped ZnO NW FETs, due to the high doping concentration, resulting in conducting NWs. As a result, we clearly confirmed that the electrical properties of ZnO NWs were systematically controlled by varying the Ga concentration.

4. CONCLUSIONS

In summary, we have fabricated controlled Ga doped ZnO NWs, by using the PVD method. We observed a good single crystalline of ZnO NWs by HR-TEM measurement. The growth direction was changed, according to the increase of Ga concentration. These results agreed well with those of XRD and PL. Ga doped ZnO NWs clearly showed a D⁰X peak without any defect emission. These results exhibited that Ga dopants in ZnO NWs were successfully doped. Also, we confirmed that the electrical properties of ZnO NWs were systematically controlled by changing Ga

concentration in the ZnO NWs. Controlled Ga-doping into ZnO NWs by the physical vapor deposition has been easily achieved, and these various Ga-doped ZnO NWs could open the possibility of new applications in nanoelectronic and nanosensing devices.

REFERENCES

- [1] Huang, M. H.; Mao, S.; Feick, H.; Yan, H.; Wu, Y.; Kind, H.; Weber, E.; Russo, R.; Yang, P. *Science*. 2001, 292, 1897 [DOI: <http://dx.doi.org/10.1126/science.1060367>].
- [2] Yan, H.; Johnson, J.; Law, M.; He, R.; Knutsen, K.; McKinney, J. R.; Pham, J.; Saykally, R.; Yang, P. *Adv. Mater.* 2003, 15, 1907 [DOI: <http://dx.doi.org/10.1002/adma.200305490>].
- [3] Könenkamp, R.; Word, R.C.; Schlegel, C. *Appl. Phys. Lett.* 2004, 85, 6004 [DOI: <http://dx.doi.org/10.1063/1.1836873>].
- [4] Wang, H. T.; Kang, B. S.; Ren, F.; Tien, L. C.; Sadik, P.W.; Norton, D. P.; Pearton, S. J.; Lin, J. *Appl. Phys. Lett.* 2005, 86, 243503 [DOI: <http://dx.doi.org/10.1063/1.1949707>].
- [5] Law, M.; Greene, L. E.; Johnson, J. C.; Saykally, R.; Yang, P. *Nature Mater.* 2005, 4, 455 [DOI: <http://dx.doi.org/10.1038/nmat1387>].
- [6] Xiong, G.; Wilkinson, J.; Mischuck, B.; Tuzemen, S.; Ucer, K. B.; Williams, R. T. *Appl. Phys. Lett.* 2002, 70, 1195.
- [7] Ma, Y.; Du, G. T.; Yang, S. R.; Li, Z. T.; Zhao, B. J.; Yang, X. T.; Yang, T. P.; Zhang, Y. T.; Liu, D. L. *J. Appl. Phys.* 2004, 95, 6268.
- [8] Jiang, X.; Wong, F. L.; Fung, M. K.; Lee, S. T. *Appl. Phys. Lett.* 2003, 83, 1875 [DOI: <http://dx.doi.org/10.1063/1.1605805>].
- [9] Yu, Z. G.; Wu, P.; Gong, H. *Appl. Phys. Lett.* 2006, 88, 132114 [DOI: <http://dx.doi.org/10.1063/1.2174089>].
- [10] Kang, H. S.; Ahn, B. D.; Kim, J. H.; Kim, G. H.; Lim, S. H.; Chang, H. W.; Lee, S. Y. *Appl. Phys. Lett.* 2006, 88, 202108 [DOI: <http://dx.doi.org/10.1063/1.2197317>].
- [11] Kim, K.; Debnath, P. C.; Park, D.-H.; Kim, S. S.; Lee, S. Y. *Appl. Phys. Lett.* 2010, 96, 083103 [DOI: <http://dx.doi.org/10.1063/1.3290247>].
- [12] Zou, C. W.; Gao, W. *Trans. Electr. Electron. Mater.* 2010, 11, 1 [DOI: <http://dx.doi.org/10.4313/TEEM.2010.11.1.001>].
- [13] Yuan, G. D.; Zhang, W. J.; Jie, J. S.; Fan, X.; Tang, J. X.; Shafiq, I.; Ye, Z. Z.; Lee, C. S.; Lee, S. T. *Adv. Mater.* 2008, 20, 168 [DOI: <http://dx.doi.org/10.1002/adma.200701377>].
- [14] Sakurai, M.; Wang, Y. G.; Uemura, T.; Aono, M. *Nanotechnology*. 2009, 20, 155203 [DOI: <http://dx.doi.org/10.1088/0957-4484/20/15/155203>].
- [15] Terasako, T.; Shirakata, S. *Jpn. J. Appl. Phys.* 2005, 44, L1410-L1413 [DOI: <http://dx.doi.org/10.1143/JJAP44.L1410>].
- [16] Lee, S. Y.; Song, Y. W.; Jeon, K. A. *J. Cryst. Growth*. 2008, 310, 4477 [DOI: <http://dx.doi.org/10.1016/j.jcrysgro.2008.07.041>].
- [17] Song, Y. W.; Lee, S. Y. *Thin Solid Films*. 2008, 518, 1323.
- [18] Goris, L.; Noriega, R.; Donovan, M.; Jokisaari, J.; Kusinski, G.; Salleo, A. *J. Electron. Mater.* 2009, 38, 586 [DOI: <http://dx.doi.org/10.1007/s11664-008-0618-x>].
- [19] Burstein, E. *Phys. Rev.* 1954, 93, 632 [DOI: <http://dx.doi.org/10.1103/PhysRev.93.632>].
- [20] Moss, T. S. *Proc. Phys. Soc. Lond.* 1954, B 67, 775.
- [21] Zhong, J.; Malcolm, S. G. *Nano. Lett.* 2006, 6, 128-132 [DOI: <http://dx.doi.org/10.1021/nl062183e>].